Taylor & Francis
Taylor & Francis Group

RESEARCH PAPER

Check for updates

SNHG17 enhances the malignant characteristics of tongue squamous cell carcinoma by acting as a competing endogenous RNA on microRNA-876 and thereby increasing specificity protein 1 expression

Xiaoming Liu, Baorong Zhang, Yue Jia, and Ming Fu

Institute of Oral Diseases, Oral Medicine Center, University of Chinese Academy of Sciences, Shenzhen Hospital, Shenzhen, Guangdong, P.R. China

ABSTRACT
A long noncoding RNA called *SNHG17* (small nucleolar RNA host gene 17) is aberrantly expressed and plays essential roles in multiple human cancer types. Nevertheless, its expression pattern and specific functions in tongue squamous cell carcinoma (TSCC) have not been well studied until now. Hence, in this study, we aimed to measure *SNHG17* expression in TSCC and to examine the actions of *SNHG17* on the malignant characteristics of TSCC cells. The regulatory mechanism that mediates the oncogenic effects of *SNHG17* on TSCC cells was investigated too. In this study, *SNHG17* was found to be upregulated in TSCC, and this overexpression closely correlated with adverse clinical parameters and shorter overall survival among the patients with TSCC. The *SNHG17* knockdown significantly decreased TSCC cell proliferation, migration, and invasion in vitro and tumor growth in vivo. Mechanism investigation revealed that *SNHG17* acts as a competing endogenous RNA on microRNA-876 (miR-876) in TSCC cells. In addition, specificity protein 1 (*SP1*) was validated as a direct target gene of miR-876 in TSCC cells. SP1 expression restoration in TSCC cells reversed miR-876 overexpression–induced anticancer effects. MiR-876 downregulation strongly attenuated the actions of the *SNHG17* knockdown in TSCC cells. *SNHG17* plays an oncogenic part in TSCC cells both in vitro and in vivo via sponging of miR-876 and thereby upregulating SP1, which could be regarded as a promising target for TSCC therapy.

Introduction

Tongue squamous cell carcinoma (TSCC) is the most prevalent subtype of oral cancer and is characterized by high malignancy, a high rate of tumor metastasis, and frequent recurrence, causing malfunctions of mastication and speech as well as dysphagia [1,2]. The morbidity rate of TSCC in China is ~4.81%, and the mortality rate of the patients is 2.21% [3]. The therapeutic methods for TSCC, including surgery, chemotherapy, and radiotherapy, advanced substantially in recent years; the TSCC-related mortality rate is still increasing, and the 5-year survival rate of the patients is only approximately 50% [4]. Over half of TSCC cases are usually detected and diagnosed at an advanced stage of this cancer; this situation is another reason for the poor clinical outcomes [5]. Thus, a better understanding of the molecular mechanisms behind the genesis and progression of TSCC may facilitate the diagnosis and treatment of this aggressive malignant tumor.

Long noncoding RNAs (lncRNAs) are a group of noncoding regulatory RNA transcripts longer than 200 nucleotides [6]. LncRNAs have no protein-coding ability but can interact with RNA, protein, and DNA [7]. In recent years, increasing evidence shows that lncRNAs play important roles in all the characteristics of physiological and pathological processes, including inflammation, differentiation, metabolism, carcinogenesis, and cancer progression [8–10]. In the field of TSCC research, a number of lncRNAs are reported to be strongly involved, eg, lncRNAs *THOR* [11], *MALAT1* [12], and *LINC00961* [13]. Aberrantly expressed lncRNAs can affect the aggressiveness of TSCC by acting as oncogenic factors or tumor suppressors [14–16]. Accordingly, investigating the expression and functions of lncRNAs in TSCC as well as their mechanisms of action may clarify the link between lncRNAs and TSCC, thus providing novel insights into TSCC management via targeting of lncRNAs.

CONTACT Xiaoming Liu ✉ liuxiaoming19931@163.com

MicroRNAs (miRNAs) are a family of endogenous, highly conserved, short noncoding RNA molecules containing 18 to 24 nucleotides [17]. They downregulate gene expression through a direct interaction with the 3′-untranslated region (3′-UTR) of complementary messenger RNAs (mRNAs, ie, target transcripts) by promoting mRNA degradation and/or inhibiting translation [18]. To date, over 2,600 miRNA genes have been confirmed in the human genome, and the encoded miRNAs are predicted to regulate the expression of ~60% of human protein-coding genes [19]. Nowadays, a growing number of studies suggest that miRNAs exert oncogenic or tumor-suppressive effects on the formation and progression of TSCC and participate in the regulation of various biological activities [20–22]. Therefore, exploration of TSCC-associated miRNAs may be useful for the identification of novel therapeutic targets in this disease.

SNHG17 is aberrantly expressed and performs important functions in multiple human cancer types [23–26]. Inspired by the above research, we tested the hypothesis that SNHG17 is involved in the progression of TSCC. To this end, we determined the expression of SNHG17 in TSCC and studied the regulatory actions of SNHG17 on the malignant phenotype of TSCC cells in vitro and in vivo. Meanwhile, the mechanisms underlying the influence of SNHG17 on TSCC progression were characterized in detail.

Materials and methods

Patients and tissue samples

A total of 56 pairs of TSCC tissue samples and adjacent non-tumor tissue samples were collected from patients at the University of the Chinese Academy of Sciences, Shenzhen Hospital between February 2013 to March 2014. All these patients had a diagnosis of primary TSCC and were treated with surgical resection. All the patients were followed-up for 5 years. Patients who had received chemotherapy and/or radiotherapy were excluded from this study. Following the surgical resection, all tissue samples were immediately immersed in liquid nitrogen and then stored at – 80°C. This study was

conducted with the approval of the Ethics Committee of the University of the Chinese Academy of Sciences, Shenzhen Hospital. All the analyzes of human subjects and their biological samples were carried out in accordance with the principles of the Helsinki Declaration. Written informed consent was provided by all the participating patients before the tissue collection.

Cell lines

Three human TSCC cell lines, Tca8113, SCC-15, and CAL-27, and normal gingival epithelial cells were bought from the American Type Culture Collection (ATCC; Manassas, VA, USA) and maintained at 37°C in an incubator supplied with 5% of CO_2. The TSCC cell lines were cultured in Dulbecco's modified Eagle's medium (DMEM) supplemented with 10% of fetal bovine serum (FBS) and 1% of a penicillin/streptomycin solution (all from Invitrogen; Thermo Fisher Scientific, Inc., Waltham, MA, USA). The normal gingival epithelial cells were grown in the Minimum Essential Medium (Invitrogen; Thermo Fisher Scientific, Inc.) supplemented with 10% of FBS and 1% of the penicillin/streptomycin solution.

Oligonucleotides, plasmids, and transient transfection

The small interfering RNA (siRNA) targeting SNHG17 (si-SNHG17) and its negative control siRNA (si-NC) were chemically synthesized by GenePharma Co., Ltd. (Shanghai, China). The full-length sequence of SP1 lacking the 3′-UTR was amplified by GenePharma Co., Ltd., and then inserted into the pcDNA3.1 vector (Invitrogen; Thermo Fisher Scientific, Inc.), resulting in a plasmid called pcDNA3.1-SP1 (pc-SP1). The miR-876 mimics, NC mimics (miR-NC), miR-876 inhibitor, and NC inhibitor were acquired from RiboBio Co., Ltd. (Guangzhou, China). To obtain different expression levels of the genes under study in cell models, one of the aforementioned oligonucleotides and one of the plasmids were transfected into cells using Lipofectamine 2000 (Invitrogen; Thermo Fisher Scientific, Inc.).

Reverse-transcription quantitative polymerase chain reaction (RT-qPCR)

Extraction of total RNA from tissues or cells was conducted by means of the TRIzol Reagent (Invitrogen; Thermo Fisher Scientific, Inc.). To assess SP1 mRNA and SNHG17 expression, the PrimeScript RT Reagent Kit (Takara Biotechnology Co., Ltd., Shiga, Japan) was applied for conversion of the total RNA into cDNA products. The resultant cDNA was then subjected to qPCR with SYBR Premix Ex Taq™ (Takara Biotechnology Co., Ltd.). GAPDH served as the internal reference control for the SP1 mRNA and SNHG17 analyses. Measurement of miR-876 expression was performed via the miScript Reverse Transcription Kit (Qiagen GmbH, Hilden, Germany) and miScript SYBR Green PCR Kit, respectively, for reverse transcription and qPCR. U6 small nuclear RNA served as a control template for miR-876. The $2^{-\Delta\Delta Ct}$ method was utilized to analyze relative expression of the genes under study [27].

Cell counting Kit-8 (CCK-8) assay

Transfected cells were collected after 24 h of incubation, were used to prepare a cell suspension, and were seeded in 96-well plates at an initial density of 2×10^3 cells per well. The cells were then maintained at 37°C and 5% CO_2 for 0, 24, 48, or 72 h, and the CCK-8 assay was carried out at the indicated time points. Another 1 h incubation was carried out with the additional 10 μl of the CCK-8 solution (Yeasen Biotechnology Co., Ltd., Shanghai, China). Absorbance was detected on a microplate reader (Bio-Rad Laboratories, Hercules, CA, USA). The growth curves were plotted with time points on the X-axis and the absorbance values on the Y-axis.

Transwell assays

The migratory status of cells was evaluated as the ability to migrate through 24-well Transwell filters (8 □m pore size; BD Biosciences, San Jose, CA, USA), whereas Matrigel (BD Biosciences)-precoated Transwell filters were employed to determine the invasiveness of cells. Following 48 h transfection, the cells were detached, washed twice with phosphate-buffered saline, and resuspended in FBS-free DMEM. A suspension containing 5×10^4 cells was inoculated into the upper compartments, whereas the lower compartments were covered with 500 μl of DMEM supplemented with 20% of FBS. All the inserts were incubated for 24 h at 37°C and 5% CO_2. Cells remaining on the upper side of the membrane were gently removed with a cotton swab, and the migratory and invasive cells were fixed with 4% paraformaldehyde and stained with 0.5% crystal violet. Images were captured by means of an inverted microscope (x200 magnification; Olympus Corporation, Tokyo, Japan). Finally, five visual fields were randomly selected, and the migratory and invasive cells were counted.

Tumor xenograft experiment

The animal experiment was conducted with the approval of the Ethics Committee of the University of the Chinese Academy of Sciences, Shenzhen Hospital. The animal experiment was carried out according to the Animal Protection Law of the People's Republic of China-2009 for experimental animals. Male BALB/c nude mice (4 to 6 weeks old) were bought from Guangdong Medical Laboratory Animal Center (Guangzhou, China) and housed in a specific-pathogen-free grade barrier environment. Cells transfected with either si-SNHG17 or si-NC were treated with 0.25% trypsin for detachment and were resuspended in phosphate-buffered saline. The cell suspension was then inoculated subcutaneously into a flank of mice. The volume of tumor xenografts was monitored and calculated via the following formula: tumor volume = ½ × length × tumor width [2]. All the mice were euthanized at 4 weeks after inoculation, and their tumor xenografts were resected, imaged, and weighed.

Bioinformatics analysis

Possible interactions between SNHG17 and miRNAs were analyzed in starBase 3.0 software (http://starbase.sysu.edu.cn/). Prediction of the potential targets of miR-876 was performed by means of starBase 3.0, TargetScan (http://www.targetscan.org/), and miRDB (http://mirdb.org/).

Nuclear/cytoplasmic fractionation

Extraction of the cytoplasmic and nuclear fractions was conducted with the PARIS Kit (Invitrogen; Thermo Fisher Scientific, Inc.).

RNA immunoprecipitation (RIP) assay

The Magna RIP RNA-Binding Protein Immunoprecipitation Kit (Millipore Inc., Billerica, MA, USA) was employed to assess the binding of miR-876 to SNHG17. In particular, a cell lysate was prepared via RIPA lysis buffer and subjected to incubation with the magnetic beads conjugated with either an anti-AGO2 antibody or control immunoglobulin G (IgG; Millipore Inc.). At the end of the experiments, the immunoprecipitated RNAs were isolated and analyzed by RT-qPCR to determine SNHG17 and miR-876 expression.

Luciferase reporter assay

The SP1 3′-UTR fragments containing the predicted wild-type (wt) or mutant (mut) miR-876–binding site were synthesized by GenePharma Co., Ltd., and inserted into the pmirGLO luciferase reporter plasmid (Promega, Madison, WI, USA) to generate reporter plasmids SP1-wt and SP1-mut, respectively. The SNHG17-wt and SNHG17-mut plasmids were constructed in a similar way. For the reporter assay, either the miR-876 mimics or miR-NC and either the wt or mut reporter plasmid were cotransfected into cells with Lipofectamine 2000. After 48 h of incubation, luciferase activity was determined with a Dual-Luciferase Reporter Assay System (Promega). Renilla luciferase activity was normalized to that of firefly luciferase.

Western blot analysis

Total protein was isolated using RIPA buffer, and protein concentration was measured with the Bicinchoninic Acid Assay Kit (both from Beyotime Institute of Biotechnology, Haimen, China). Equal amounts of protein were loaded and resolved by SDS-PAGE on a 10% gel and then transferred onto polyvinylidene difluoride (PVDF) membranes. After blockage with 5% fat-free milk at room temperature for 2 h, the membranes were probed with primary antibodies against SP1 (cat. No. ab124804; dilution 1:1,000; Abcam, Cambridge, UK) or GAPDH (cat. No. ab181602; dilution 1:1,000; Abcam), followed by incubation with a goat anti-rabbit IgG antibody conjugated with horseradish peroxidase secondary antibody (cat. No. ab205718; dilution 1:5,000; Abcam). The protein signals were developed with the Pierce ECL Western Blotting Substrate (Pierce; Thermo Fisher Scientific, Inc.). GAPDH served as the loading control.

Statistical analysis

Each experiment was performed for at least three times. All results are presented as the mean ± standard deviation and were analyzed using the SPSS software (version 19.0; SPSS Inc.). The correlation between SNHG17 expression and the clinical parameters among the 56 patients with TSCC was assessed by the χ^2 test. Differences between two groups were evaluated by Student's t test; one-way analysis of variance in combination with Tukey's post hoc test was conducted to compare the data among multiple groups. The association between SNHG17 expression and overall survival of TSCC patients was analyzed via the Kaplan–Meier curve and logrank test. Data with $P < 0.05$ were considered statistically significant.

Results

High expression of SNHG17 correlates with poor clinical outcomes of patients with TSCC

First, RT-qPCR was carried out to measure SNHG17 expression in the 56 pairs of TSCC tumors and adjacent non-tumor tissue samples. The results indicated that the expression of SNHG17 was higher in TSCC tissue samples than in the adjacent non-tumor tissue samples (Figure 1(a), $p < 0.05$). Consistently with this result, SNHG17 expression was higher in all three TSCC cell lines (Tca8113, SCC-15, and CAL-27) than in the normal gingival epithelial cells (Figure 1(b), $p < 0.05$).
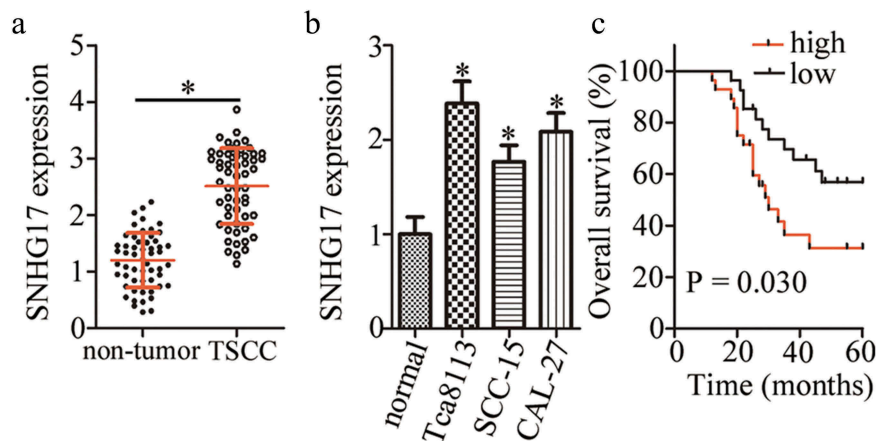
Figure 1. Expression of *SNHG17* is excessive in TSCC tissue samples and cell lines. (a) RT-qPCR analysis was performed to determine *SNHG17* expression in 56 pairs of TSCC tissue samples and adjacent non-tumor tissues. *P < 0.05 vs. non-tumor tissue samples. (b) *SNHG17* expression was analyzed via RT-qPCR in three TSCC cell lines and normal gingival epithelial cells. *P < 0.05 vs. normal gingival epithelial cells. (c) Kaplan–Meier analysis and logrank test revealed that patients with TSCC harboring *SNHG17* over-expression exhibited obviously shorter overall survival when compared with the group with low *SNHG17* expression. P = 0.030.

We next investigated the clinical value of aberrant *SNHG17* expression in patients with TSCC. The median value of *SNHG17* among the TSCC tissue samples was defined as the cutoff value (2.74), and according to the cutoff, all the patients with TSCC were subdivided into either a high *SNHG17* expression group (n = 28) or low *SNHG17* expression group (n = 28). The χ^2 test indicated that higher *SNHG17* expression notably correlated with tumor size (P = 0.015), TNM stage (P = 0.029) and lymph node metastasis (P = 0.031) among the 56 patients with TSCC (Table 1). In addition, patients with TSCC featuring high TSCC expression showed shorter overall survival compared with that in the group with low *SNHG17*

expression (Figure 1(c), p = 0.030). These findings suggested that *SNHG17* expression is high in TSCC, and this overexpression may be associated with TSCC progression.

The knockdown of SNHG17 inhibits the proliferation, migration, and invasiveness of Tca8113 and CAL-27 cells

The expression of *SNHG17* was higher in Tca8113 and CAL-27 cells among the three TSCC cell lines; accordingly, these two cell lines were chosen for subsequent functional assays. *SNHG17* expression was silenced in Tca8113 and CAL-27 cells using the siRNA called si-SNHG17. RT-qPCR confirmed that *SNHG17* was remarkably downregulated in the Tca8113 and CAL-27 cells that were transfected with si-SNHG17 (Figure 2(a), p < 0.05). The CCK-8 assay revealed that the transfection of si-SNHG17 obviously decreased the proliferative ability of Tca8113 and CAL-27 cells (Figure 2(b), p < 0.05). We then tested whether the reduction in *SNHG17* expression affects the migration and invasiveness of TSCC cells. The results of Transwell assays meant that the migratory (Figure 2(c), p < 0.05) and invasive (Figure 2(d), p < 0.05) abilities were notably hindered in the Tca8113 and CAL-27 cells with the *SNHG17* knockdown. The above results showed that *SNHG17* may play a tumor-suppressive part in the malignancy of TSCC.

Table 1. Correlation between *SNHG17* expression and clinical characteristics in patients with TSCC.

| Clinical characteristics	SNHG17 expression		
	High	Low	P
Age (years)			0.412
< 55	19 (67.9%)	15 (53.6%)	
≥ 55	9 (32.1%)	13 (46.4%)	
Gender			0.591
Male	14 (50.0%)	17 (60.7%)	
Female	14 (50.0%)	11 (39.3%)	
Tumor size (cm)			0.015*
< 2	8 (28.6%)	18 (64.3%)	
≥ 2	20 (71.4%)	10 (35.7%)	
TNM stage			0.029*
I-II	12 (42.9%)	21 (75.0%)	
III-IV	16 (57.1%)	7 (25.0%)	
Lymph node metastasis			0.031*
Absence	10 (35.7%)	19 (67.9%)	
Presence	18 (64.3%)	9 (32.1%)	

*P < 0.05 by χ^2 test.
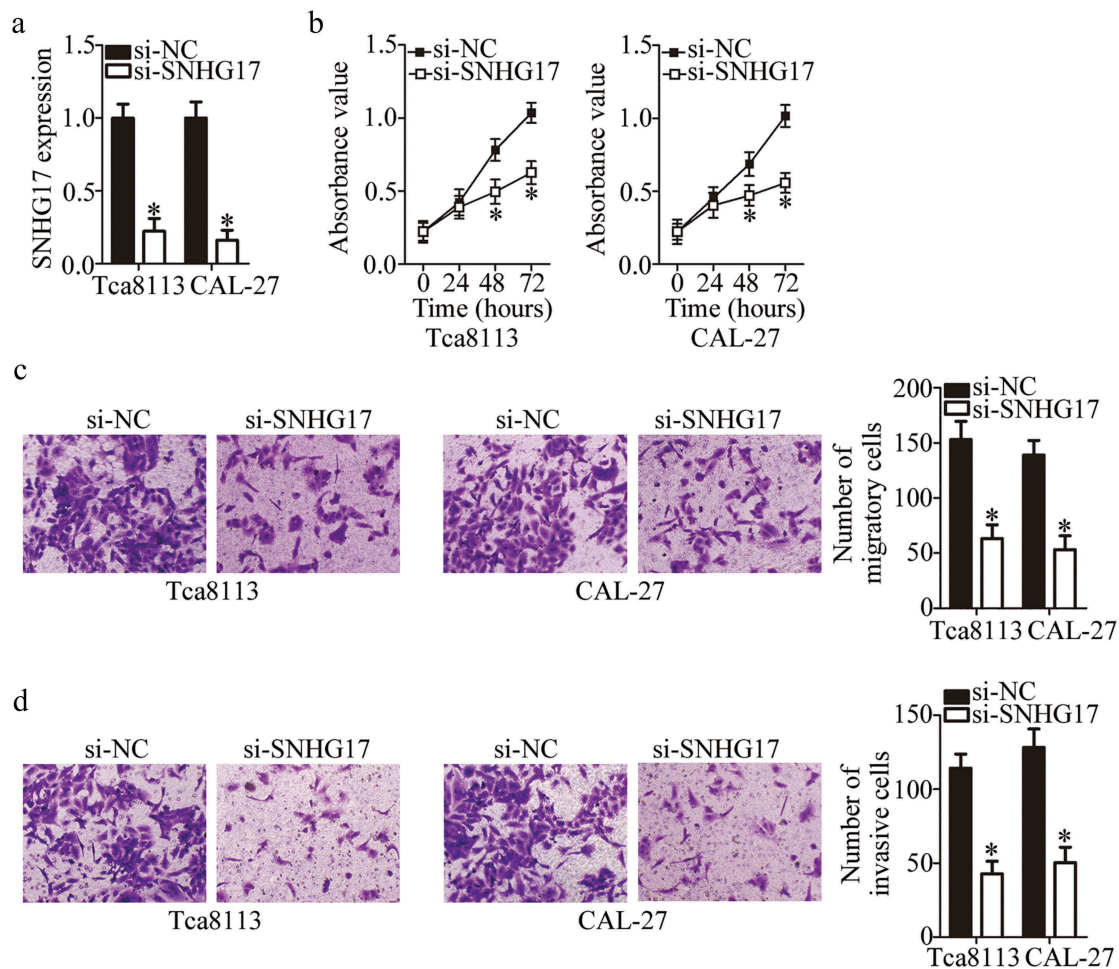
Figure 2. The knockdown of *SNHG17* attenuates the malignant characteristics of Tca8113 and CAL-27 cells. Tca8113 and CAL-27 cells were transfected with either si-SNHG17 or si-NC. The transfected cells were collected and used in the subsequent experiments. (a) Transfected cells were collected after 48 h cultivation. Total RNA was extracted and then subjected to RT-qPCR analysis for the determination of transfection efficiency. *P < 0.05 vs. the si-NC group. (b) The CCK-8 assay was performed to quantitate the proliferation of Tca8113 and CAL-27 cells after si-SNHG17 or si-NC transfection. Absorbance was measured at time points 0, 24, 48, and 72 h after cell seeding. *P < 0.05 vs. group si-NC. (c, d) The effects of the *SNHG17* knockdown on the migration and invasiveness of Tca8113 and CAL-27 cells were investigated in Transwell assays. *P < 0.05 vs. group si-NC.

SNHG17 acts as a sponge on miR-876 in TSCC cells

Currently, the most widely accepted theory is that the cytoplasmic lncRNAs work as a competing endogenous RNA (ceRNA) by sponging certain miRNAs and thereby enhancing the expression of these miRNAs' targets [28]. To reveal the molecular events underlying the oncogenic influence of *SNHG17* on TSCC progression, we first determined the subcellular localization of *SNHG17* in Tca8113 and CAL-27 cells. As depicted in Figure 3(a), *SNHG17* was mostly present in the cytoplasm of both Tca8113 and CAL-27 cells. Bioinformatics software starBase 3.0 was applied to search for the potential miRNAs that may be sponged by *SNHG17*. The bioinformatics prediction uncovered

complementary sequences between *SNHG17* and miR-876 (Figure 3(b)). MiR-876 was selected for subsequent validation because this miRNA has been demonstrated to exert important actions on tumorigenesis and tumor progression [29–34]. The luciferase reporter assay was performed to investigate whether miR-876 can bind to *SNHG17*. The miR-876 mimics–mediated overexpression of miR-876 (Figure 3(c), p < 0.05) significantly decreased the luciferase activity of SNHG17-wt in Tca8113 and CAL-27 cells (P < 0.05), but upregulation of miR-876 had no influence on the luciferase activity of SNHG17-mut (Figure 3(d)).

The RIP assay was conducted to gain more insight into the interaction between *SNHG17* and miR-876 in TSCC cells. The results showed that *SNHG17* and
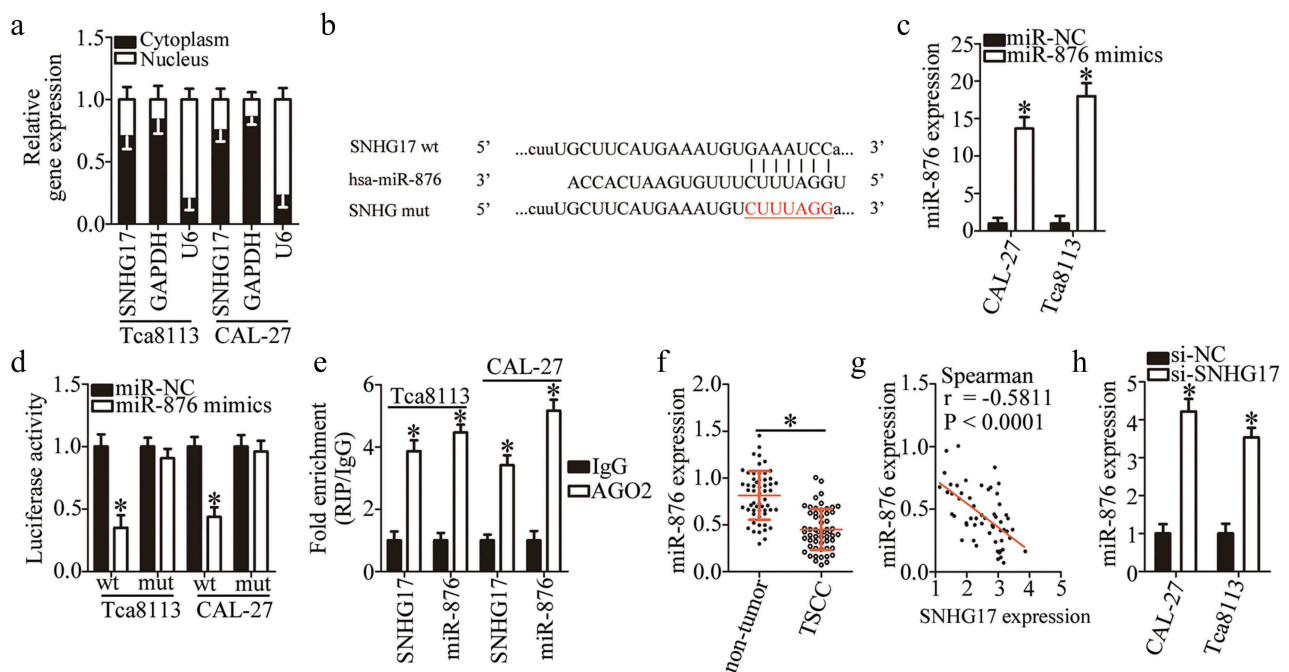
Figure 3. *SNHG17* serves as a ceRNA of miR-876 in TSCC cells. (a) *SNHG17* expression in nuclear and cytoplasmic fractions of Tca8113 and CAL-27 cells was evaluated and indicated that *SNHG17* was mostly present in the cytoplasm. (b) The wt binding site for miR-876 in the *SNHG17* constructs, as predicted by starBase 3.0. The mutant binding sequences are shown too. (c) The expression of miR-876 in miR-876 mimics–transfected or miR-NC–transfected Tca8113 and CAL-27 cells was measured via RT-qPCR. *P < 0.05 vs. the miR-NC group. (d) The luciferase reporter assay was carried out to confirm the interaction between miR-876 and *SNHG17* in TSCC cells. The luciferase activity of Tca8113 and CAL-27 cells was analyzed via a Dual-Luciferase Reporter Assay System after cotransfection with either the miR-876 mimics or miR-NC and either SNHG17-wt or SNHG17-mut. *P < 0.05 vs. group miR-NC. (e) RIP assay results on the physical association between miR-876 and *SNHG17* in Tca8113 and CAL-27 cells. *P < 0.05 vs. the IgG group. (f) MiR-876 expression in the 56 pairs of TSCC tissue samples and adjacent non-tumor tissues was determined by RT-qPCR. *P < 0.05 vs. adjacent non-tumor tissues. (g) The expression correlation between miR-876 and *SNHG17* in the 56 TSCC tissue samples was studied by Spearman's correlation analysis. r = −0.5811, P < 0.0001. (h) The expression of miR-876 in *SNHG17*-depleted Tca8113 and CAL-27 cells was tested by RT-qPCR. *P < 0.05 vs. group si-NC.

miR-876 were preferentially enriched on AGO2-binding beads after immunoprecipitation in the lysates of Tca8113 and CAL-27 cells, suggesting that miR-876 is a target of *SNHG17* in TSCC cells (Figure 3(e)), p < 0.05. Furthermore, the expression of miR-876 was measured in the 56 pairs of TSCC tissue samples and adjacent non-tumor tissues, and expression correlation with *SNHG17* was evaluated. The data revealed that miR-876 was underexpressed in TSCC tumors (Figure 3(f), p < 0.05), manifesting an inverse correlation with *SNHG17* amounts (Figure 3(g); r = −0.5811, P < 0.0001). Moreover, miR-876 turned out to be significantly upregulated in *SNHG17* knockdown Tca8113 and CAL-27 cells, as evidenced by RT-qPCR analysis (Figure 3(h), p < 0.05). Consequently, *SNHG17* functioned as a molecular sponge of miR-876 thereby inhibiting miR-876 function in TSCC.

MiR-876 overexpression exerts inhibitory effects on the proliferation, migration, and invasiveness of Tca8113 and CAL-27 cells

To investigate whether miR-876 is associated with TSCC progression, a series of experiments was conducted on miR-876–overexpressing Tca8113 and CAL-27 cells. The CCK-8 assay showed that miR-876 mimics–transfected Tca8113 and CAL-27 cells manifested slower proliferation compared with that of the cells transfected with miR-NC (Figure 4(a), p < 0.05). Furthermore, the Transwell assay results revealed that ectopic miR-876 expression obviously restricted the migration (Figure 4(b), p < 0.05) and invasiveness (Figure 4 (c), p < 0.05) of Tca8113 and CAL-27 cells. These data implied that miR-876 acted as tumor-suppressive miRNA on TSCC progression.
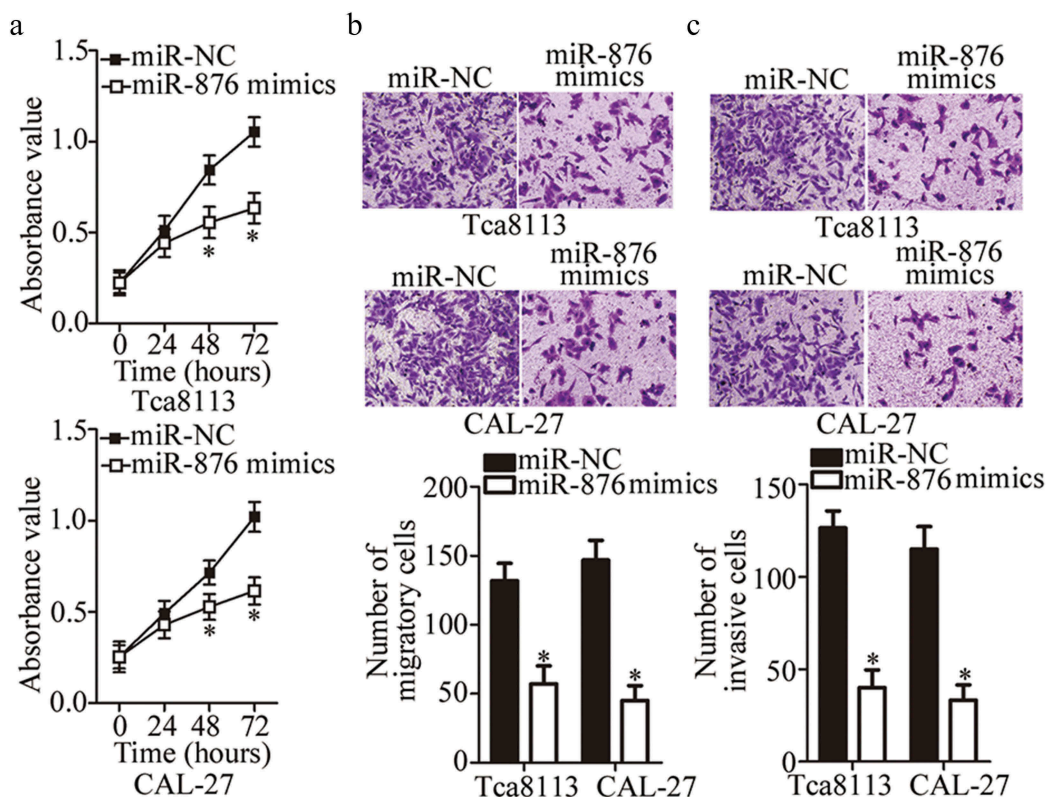
Figure 4. Overexpression of miR-876 significantly decreases the proliferation, migration, and invasiveness of Tca8113 and CAL-27 cells. (a) The CCK-8 assay was conducted to evaluate the proliferative ability of miR-876–overexpressing Tca8113 and CAL-27 cells. *P < 0.05 vs. the miR-NC group. (b, c) The migratory and invasive abilities of Tca8113 and CAL-27 cells that were transfected with either the miR-876 mimics or miR-NC were assessed by Transwell assays. *P < 0.05 vs. group miR-NC.

MiR-876 directly targets SP1 mRNA in TSCC cells

To decipher the molecular mechanisms via which miR-876 reduces the malignancy of TSCC cells, potential targets of miR-876 were predicted by means of starBase 3.0, TargetScan, and miRDB. Two highly conserved possible miR-876–binding sites were found in the 3′-UTR of SP1 mRNA (Figure 5(a)). The luciferase reporter assay was conducted to test whether miR-876 can directly bind to the 3′-UTR of SP1 mRNA. The luciferase activity was noticeably lower in SP1-wt–transfected (1 and 2) Tca8113 and CAL-27 cells that were cotransfected with the miR-876 mimics (P < 0.05); however, no suppression of the luciferase activity was observed among the cells that were transfected with SP1-mut instead (both 1 and 2; Figure 5(b)).

Besides, RT-qPCR was performed to determine SP1 mRNA expression in the 56 pairs of TSCC tissue samples and adjacent non-tumor tissues. The mRNA of SP1 was found to be overexpressed in the TSCC tumors in comparison with that in the adjacent non-tumor tissues

(Figure 5(c), p < 0.05). In addition, among the TSCC tissue samples, the expression levels of miR-876 and of SP1 mRNA correlated inversely (Figure 5(d); r = −0.5992, P < 0.0001). RT-qPCR and western blotting suggested that transfection with the miR-876 mimics caused prominent downregulation of SP1 mRNA (Figure 5(e), p < 0.05) and protein (Figure 5(f), p < 0.05) in Tca8113 and CAL-27 cells. These results proved that SP1 mRNA is a direct target of miR-876 in TSCC cells.

Restoration of SP1 expression abrogates the tumor-suppressive effects of miR-876 on TSCC cells

On the basis of the above observations, it was hypothesized that miR-876 upregulation attenuated the growth and metastasis of TSCC cells by decreasing SP1 expression. To test this hypothesis, rescue experiments were performed on miR-876–overexpressing Tca8113
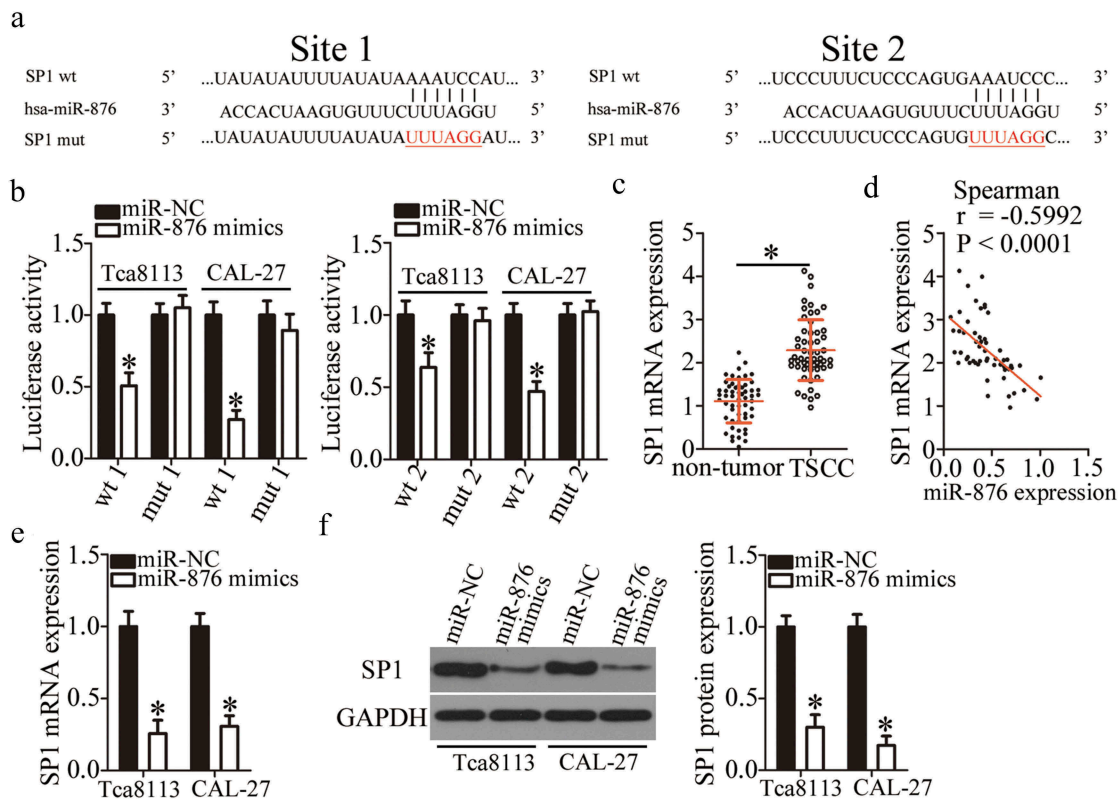
Figure 5. *SP1* is a direct target gene of miR-876 in TSCC cells. (a) The wt and mutant miR-876–binding sequences in the 3′-UTR of *SP1* mRNA. (b) Either SP1-wt or SP1-mut and either the miR-876 mimics or miR-NC were introduced into Tca8113 and CAL-27 cells. Luciferase activity was determined at 48 h after the transfection. *P < 0.05 vs. group miR-NC. (c) The mRNA levels of SP1 in the 56 pairs of TSCC tissue samples and adjacent non-tumor tissues were quantified via RT-qPCR. *P < 0.05 vs. adjacent non-tumor tissues. (d) Spearman's analysis of correlation between the expression levels of miR-876 and SP1 in the 56 TSCC tumors. r = −0.5992, P < 0.0001. (e, f) The SP1 mRNA and protein amounts in miR-876–overexpressing Tca8113 and CAL-27 cells were quantitated respectively through RT-qPCR and western blotting. *P < 0.05 vs. miR-NC.

and CAL-27 cells via cotransfection with the SP1-overexpressing plasmid (pc-SP1). Western blotting confirmed that the SP1 protein was significantly downregulated in miR-876–overexpressing Tca8113 and CAL-27 cells; meanwhile, cotransfection with pc-SP1 almost abrogated the SP1 protein downregulation that was caused by miR-876 overexpression (Figure 6(a), p < 0.05). Furthermore, a series of functional assays indicated that restoration of SP1 expression abrogated the inhibitory effects of miR-876 overexpression on the proliferation (Figure 6(b), p < 0.05), migration (Figure 6 (c), p < 0.05), and invasiveness (Figure 6(d), p < 0.05) of Tca8113 and CAL-27 cells in vitro. These data suggested that the decrease in SP1 expression is essential for the inhibitory actions of miR-876 on the malignancy of TSCC cells.

The miR-876–SP1 axis is involved in SNHG17-driven stimulation of TSCC cell proliferation, migration, and invasion

On the basis of the above results, it was hypothesized that the *SNHG17* knockdown inhibits the proliferation, migration, and invasiveness of TSCC cells via downregulation of the miR-876–SP1 axis output. Hence, rescue experiments were conducted to validate this notion. First, the transfection efficiency was evaluated by RT-qPCR. It was noted that miR-876 expression was markedly silenced in Tca8113 and CAL-27 cells by miR-876 inhibitor transfection (Figure 7(a), p < 0.05). Then, si-SNHG17 and either the miR-876 inhibitor or NC inhibitor were introduced into Tca8113 and CAL-27 cells. The downregulation of *SNHG17* increased miR-876 expression (Figure 7(b), p < 0.05) and decreased SP1 protein amounts (Figure 7 (c), p < 0.05) in Tca8113 and CAL-27 cells, whereas miR-
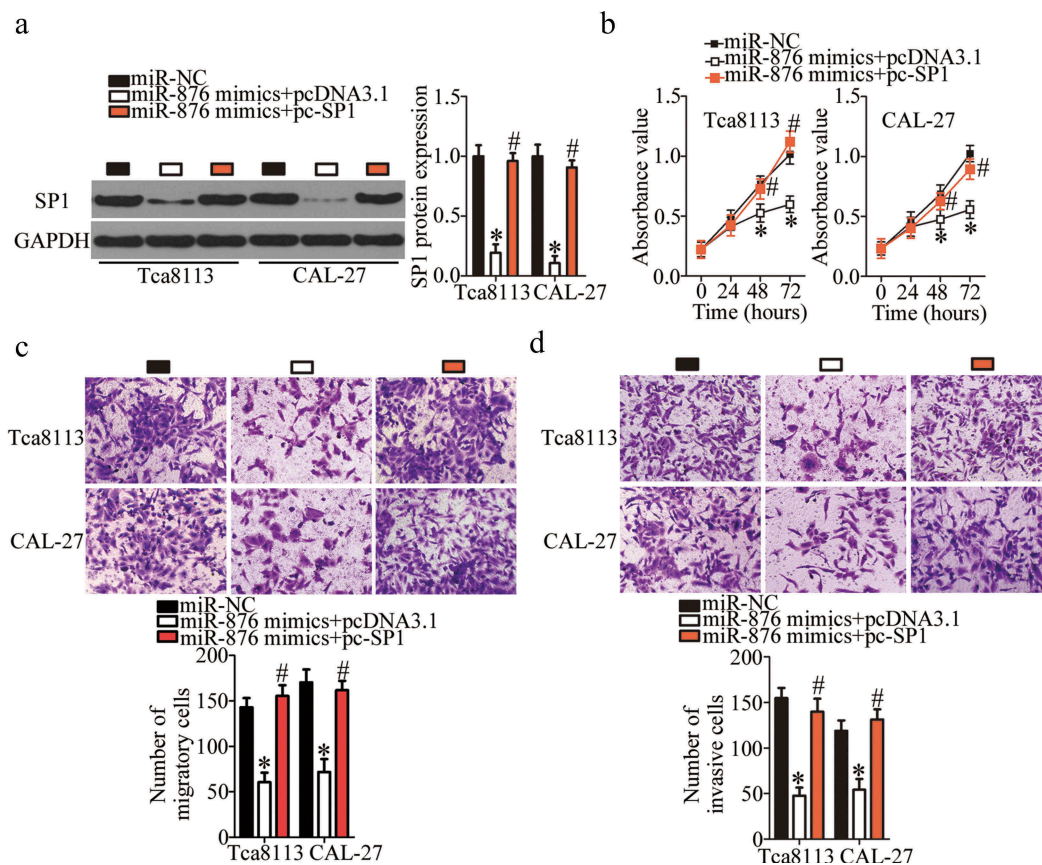
Figure 6. Restoration of SP1 expression abrogates the inhibitory influence of miR-876 overexpression on Tca8113 and CAL-27 cell proliferation, migration, and invasion. (a) Western blotting was performed to measure the protein levels of SP1 in Tca8113 and CAL-27 cells after cotransfection with the miR-876 mimics and either pc-SP1 or pcDNA3.1. *P < 0.05 vs. the miR-NC group. #P < 0.05 vs. group miR-876 mimics+pcDNA3.1. (b–d) The proliferation, migration, and invasiveness of the aforementioned cells were investigated in CCK-8 and Transwell assays, respectively. *P < 0.05 vs. the miR-NC group. #P < 0.05 vs. group miR-876 mimics+pcDNA3.1.

876 inhibitor treatment abrogated these effects. CCK-8 and Transwell assays next revealed that the proliferation (Figure 7(d), p < 0.05), migration (Figure 7(e), p < 0.05), and invasiveness (Figure 7(f), p < 0.05) of Tca8113 and CAL-27 cells were notably suppressed by the *SNHG17* knockdown, and conversely, these effects were reversed after cotransfection with the miR-876 inhibitor. In short, all these findings led to a conclusion that the *SNHG17* knockdown restricted TSCC progression in vitro by reducing the sponging of miR-876, with a consequent decrease in SP1 expression.

The SNHG17 knockdown impairs tumor growth of TSCC cells in vivo

The tumor xenograft experiment was carried out to corroborate the oncogenic effect of *SNHG17* in TSCC more comprehensively. Tca8113 cells transfected with either si-SNHG17 or si-NC were harvested and then injected subcutaneously into the flank of mice. The volume of tumor xenografts was monitored, and these data were used for plotting the tumor growth curve. It was observed that the growth rate of tumor xenografts was markedly slower in the si-SNHG17 group than in the si-NC group (Figure 8(a), p < 0.05). At 4 weeks after the inoculation, all the mice were euthanized. The tumor xenografts from the si-SNHG17 and si-NC groups are illustrated in Figure 8(b). In addition, the tumor xenografts originating from the Tca8113 cells transfected with si-SNHG17 manifested a lower weight compared with that in the si-NC group (Figure 8(c), p < 0.05).

Furthermore, we determined the expression of *SNHG17*, miR-876, and SP1 in the tumor xenografts. RT-qPCR revealed that *SNHG17* expression was lower (Figure 8(d), p < 0.05) while miR-876 expression was higher (Figure 8(e), p < 0.05) in the tumor xenografts derived from si-
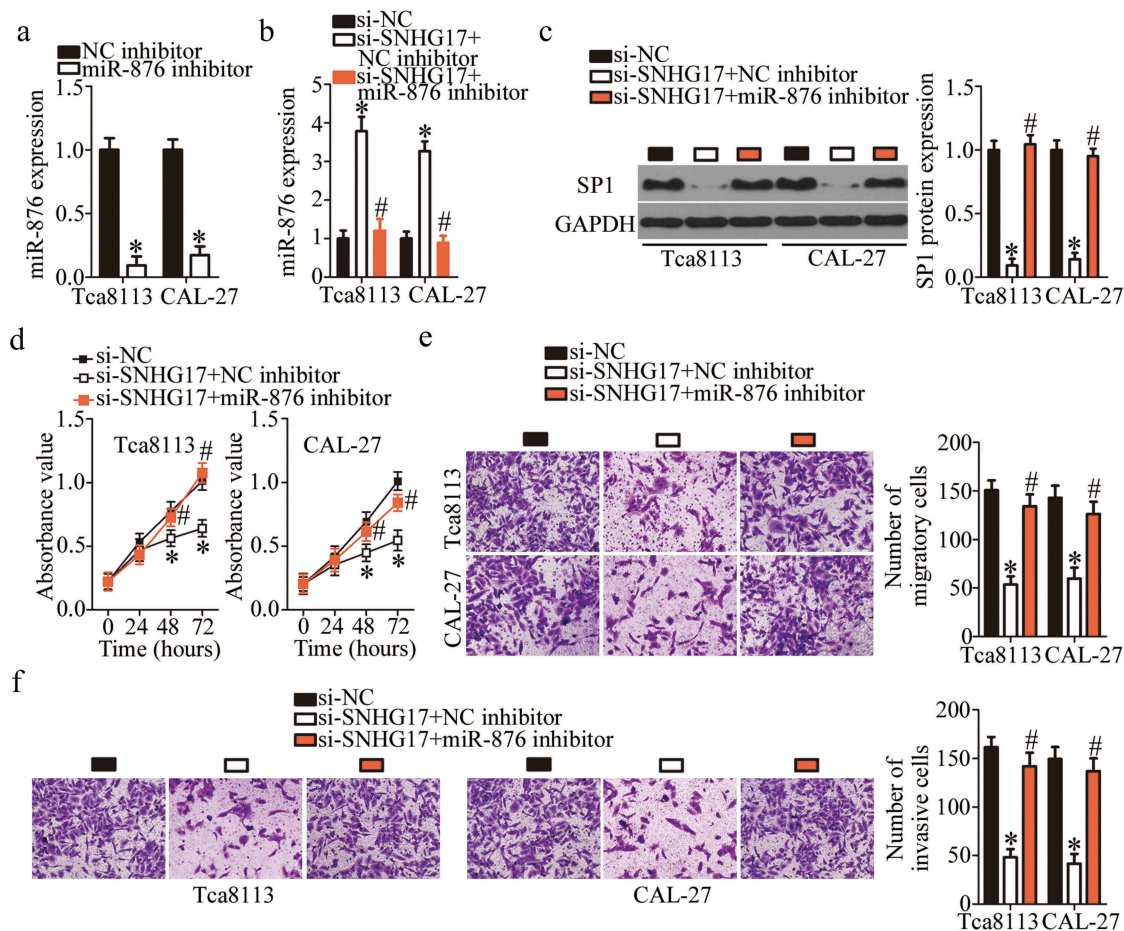
Figure 7. The *SNHG17* knockdown inhibits the proliferation, migration, and invasiveness of Tca8113 and CAL-27 cells via modulation of the miR-876–SP1 axis. (a) Either the miR-876 inhibitor or NC inhibitor was transfected into Tca8113 and CAL-27 cells. RT-qPCR was applied to measure miR-876 expression at 48 h post-transfection. *P < 0.05 vs. the NC inhibitor group. (b, c) The expression of the miR-876 and SP1 protein in Tca8113 and CAL-27 cells – that were cotransfected with si-SNHG17 and either the miR-876 inhibitor or NC inhibitor – was respectively determined by RT-qPCR and western blotting. *P < 0.05 vs. group si-NC. #P < 0.05 vs. group si-SNHG17+ NC inhibitor. (d–f) CCK-8 and Transwell assays were performed to examine the proliferation, migration, and invasiveness of Tca8113 and CAL-27 cells that were treated as described above. *P < 0.05 vs. the si-NC group. #P < 0.05 vs. group si-SNHG17+ NC inhibitor.

SNHG17–transfected Tca8113 cells. Furthermore, western blotting results suggested that the protein amount of SP1 was lower in the si-SNHG17 group than in the si-NC group (Figure 8(f)). Therefore, these results meant that a reduction in *SNHG17* expression restrained tumor growth in vivo by regulating the miR-876–SP1 axis.

Discussion

A variety of lncRNAs are aberrantly expressed in TSCC, and their anomalous expression has been extensively demonstrated to play crucial roles in TSCC progression [35–37]. LncRNAs have tumor-suppressive or oncogenic functions and are implicated

in the regulation of diverse cancer-related abnormal cellular behaviors [38–40]. Hence, in-depth research into the functional involvement of lncRNAs in TSCC may help to identify diagnostic or prognostic biomarkers of (and therapeutic targets in) TSCC. In this work, we first measured the expression of *SNHG17* in TSCC and evaluated its clinical significance among the 56 patients with TSCC. Additionally, we investigated the interactions of *SNHG17* with the miRNA–mRNA axis in relation to the regulation of aggressive characteristics of TSCC cells. This study illustrates a novel lncRNA–miRNA–mRNA pathway that contributes to the malignant phenotype of TSCC.

SNHG17 is overexpressed in gastric cancer, and its upregulation is closely associated with invasion
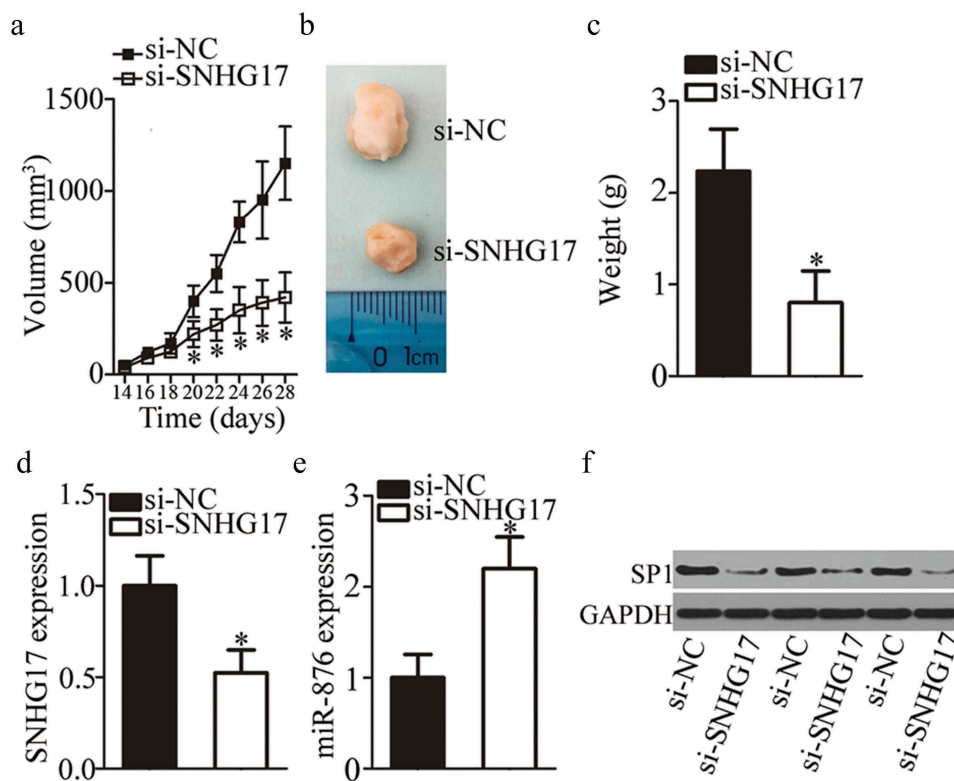
Figure 8. The knockdown of *SNHG17* inhibits tumor growth of TSCC cells in vivo. (a) Nude mice were injected with Tca8113 cells that were transfected with either si-SNHG17 or si-NC. The growth curve was plotted with the tumor volume on the Y-axis and time (days) on the X-axis. *P < 0.05 vs. group si-NC. (b) Representative images of tumor xenografts derived from the mice inoculated with either si-SNHG17–transfected or si-NC–transfected Tca8113 cells. (c) Weight of the tumor xenografts was determined at 4 weeks after injection. *P < 0.05 vs. group si-NC. (d, e) Total RNA was isolated from tumor xenografts and was subjected to the quantification of *SNHG17* and miR-876 expression. *P < 0.05 vs. the si-NC group. (f) The protein level of SP1 in tumor xenografts was assessed by western blotting.

depth, TNM stage, lymph node metastasis, and distant metastasis [23,24]. Patients with gastric cancer harboring *SNHG17* overexpression exhibit worse overall survival and progression-free survival than do the patients with low *SNHG17* expression [23]. Of note, *SNHG17* expression has been identified as an independent biomarker predicting the overall survival and progression-free survival of patients with gastric cancer [23]. *SNHG17* expression is also excessive in colorectal cancer [25] and non–small cell lung cancer [26]. Nonetheless, the expression status of *SNHG17* in TSCC has been unclear. Herein, a total of 56 pairs of TSCC tissue samples and adjacent non-tumor tissue samples were collected and assayed by RT-qPCR to quantitate *SNHG17* expression. The results showed that *SNHG17* is overexpressed in TSCC, and this overexpression correlated with tumor size, TNM stage and lymph node metastasis. Patients with TSCC featuring high *SNHG17*

expression showed shorter overall survival in comparison with the patients with low *SNHG17* expression. These results suggest that *SNHG17* might be a diagnostic and/or prognostic biomarker of TSCC.

Previously, *SNHG17* has been validated as an oncogenic lncRNA in carcinogenesis and cancer progression. For instance, silencing of *SNHG17* expression suppresses colorectal-cancer cell proliferation in vitro, promotes apoptosis and cell cycle arrest in vitro, and slows tumor growth of colorectal-cancer cells in vivo [25]. In non–small cell lung cancer, *SNHG17* downregulation restricts tumor cell proliferation and migration and induces apoptosis in vitro [26].However, the specific participation of *SNHG17* in TSCC has not yet been elucidated. In this study, a series of functional experiments revealed that *SNHG17* downregulation causes evident suppression of TSCC cell proliferation, migration, and invasion in vitro and

their tumor growth in vivo. These observations suggest that *SNHG17* may be an effective target for managing TSCC.

Our identification of the mechanism of *SNHG17* action should advance the understanding of its involvement in cancer initiation and progression. Previously, the oncogenic roles of *SNHG17* have been convincingly attributed to an epigenetic knockdown of P57 in colorectal cancer [25] and to regulation of FOXA1, XAF1, and BIK expression in non–small cell lung cancer [26]. In the present study, we demonstrated that *SNHG17* works as a ceRNA of miR-876 in TSCC and thereby relieves the repressive action of miR-876 on its direct target gene, *SP1*. MiR-876 is known to be downregulated in hepatocellular carcinoma [29], breast cancer [30,31], gastric cancer [32], osteosarcoma [33], and lung cancer [34]. MiR-876 plays tumor-suppressive roles and participates in the regulation of a variety of cancer-associated processes in human malignant tumors [29–34]. To the best of our knowledge, the present study is the first to show that miR-876 is sponged by *SNHG17* and may therefore inhibit the malignancy of TSCC cells.

SP1, a sequence-specific DNA-binding protein, is encoded by a gene in chromosomal region 12q13.1 [41]. SP1 can directly interact with GC/GT-rich promoter elements via its C(2)H(2)-type zinc fingers at C-terminal domains and subsequently enhances or attenuates the activity of gene promoters [42]. SP1 expression is high in a variety of human malignant tumors, including prostate cancer [43], breast cancer [44], gastric cancer [45], and thyroid cancer [46]. In TSCC, SP1 is overexpressed too and significantly promotes the genesis and progression of TSCC by regulating numerous cellular behaviors [47–49] in agreement with our findings. In this study, our data uncovered a novel upstream molecular mechanism controlling the expression of SP1 in TSCC. Namely, *SNHG17* acts as a ceRNA on miR-876 and thus upregulates SP1 in TSCC cells. Consequently, the *SNHG17*–miR-876–SP1 pathway facilitates TSCC progression in vitro and in vivo, highlighting promising targets for TSCC therapy.

Conclusion

We demonstrated that *SNHG17* serves as a sponge of miR-876 in TSCC thereby weakening the inhibitory action of miR-876 on *SP1* expression and driving aggressive TSCC progression. The components of this regulatory pathway, including *SNHG17*, miR-876, and SP1, are potential targets for the development of novel therapies for TSCC.

Disclosure statement

No potential conflict of interest was reported by the authors.

References

[1] Tanaka T, Tanaka M, Tanaka T. Oral carcinogenesis and oral cancer chemoprevention: a review. Patholog Res Int. 2011;2011:431246.

[2] Zhang T, Lubek JE, Salama A, et al. Treatment of cT1N0M0 tongue cancer: outcome and prognostic parameters. J Oral Maxillofacial Surg. 2014;72:406–414.

[3] Chen W, Zheng R, Baade PD, et al. Cancer statistics in China, 2015. CA Cancer J Clin. 2016;66:115–132.

[4] Patel SG, Amit M, Yen TC, et al. Lymph node density in oral cavity cancer: results of the International Consortium for Outcomes Research. Br J Cancer. 2013;109:2087–2095.

[5] Yuen PW, Lam KY, Chan AC, et al. Clinicopathological analysis of local spread of carcinoma of the tongue. Am J Surg. 1998;175:242–244.

[6] Evans JR, Feng FY, Chinnaiyan AM. The bright side of dark matter: lncRNAs in cancer. J Clin Invest. 2016;126:2775–2782.

[7] Lu Q, Yu T, Ou X, et al. Potential lncRNA diagnostic biomarkers for early gastric cancer. Mol Med Rep. 2017;16:9545–9552.

[8] Quinn JJ, Chang HY. Unique features of long non-coding RNA biogenesis and function. Nat Rev Genet. 2016;17:47–62.

[9] Beermann J, Piccoli MT, Viereck J, et al. Non-coding RNAs in development and disease: background, mechanisms, and therapeutic approaches. Physiol Rev. 2016;96:1297–1325.

[10] Feng W, Zong W, Li Y, et al. Abnormally expressed long noncoding RNA B3GALT5-AS1 may serve as a biomarker for the diagnostic and prognostic of gastric cancer. J Cell Biochem. 2020 Jan;121(1):557–565.

[11] Yang H, Fu G, Liu F, et al. LncRNA THOR promotes tongue squamous cell carcinomas by stabilizing IGF2BP1 downstream targets. Biochimie. 2019;165:9–18.

[12] Zhu M, Zhang C, Chen D, et al. lncRNA MALAT1 potentiates the progression of tongue squamous cell

carcinoma through regulating miR-140-5p-PAK1 pathway. Onco Targets Ther. 2019;12:1365–1377.

[13] Zhang L, Shao L, Hu Y. Long noncoding RNA LINC00961 inhibited cell proliferation and invasion through regulating the Wnt/beta-catenin signaling pathway in tongue squamous cell carcinoma. J Cell Biochem. 2019;120:12429–12435.

[14] Zhang S, Ma H, Zhang D, et al. LncRNA KCNQ1OT1 regulates proliferation and cisplatin resistance in tongue cancer via miR-211-5p mediated Ezrin/Fak/Src signaling. Cell Death Dis. 2018;9:742.

[15] Ren Y, He W, Chen W, et al. CRNDE promotes cell tongue squamous cell carcinoma cell growth and invasion through suppressing miR-384. J Cell Biochem. 2019;120:155–163.

[16] Li Y, Wan Q, Wang W, et al. LncRNA ADAMTS9-AS2 promotes tongue squamous cell carcinoma proliferation, migration and EMT via the miR-600/EZH2 axis. Biomed Pharmacothe. 2019;112:108719.

[17] Gomes CC, Gomez RS. MicroRNA and oral cancer: future perspectives. Oral Oncol. 2008;44:910–914.

[18] Grange C, Collino F, Tapparo M, et al. Oncogenic micro-RNAs and renal cell carcinoma. Front Oncol. 2014;4:49.

[19] Friedman RC, Farh KK, Burge CB, et al. Most mammalian mRNAs are conserved targets of microRNAs. Genome Res. 2009;19:92–105.

[20] Karatas OF, Oner M, Abay A, et al. MicroRNAs in human tongue squamous cell carcinoma: from pathogenesis to therapeutic implications. Oral Oncol. 2017;67:124–130.

[21] Yu X, Li Z. MicroRNA expression and its implications for diagnosis and therapy of tongue squamous cell carcinoma. J Cell Mol Med. 2016;20:10–16.

[22] Ma T, Zhao Z, Wang Z, et al. MiR-940 inhibits migration and invasion of tongue squamous cell carcinoma via regulatingCXCR2/NF-kappaB system-mediated epithelial-mesenchymal transition. Naunyn-Schmiedeberg's Arch Pharmacol. 2019;392:1359–1369.

[23] Chen LL, He J, Qiu XT, et al. The prognostic roles of long non-coding RNA SNHG17 in the patients with gastric cancer. Eur Rev Med Pharmacol Sci. 2019;23:1063–1068.

[24] Zhang G, Xu Y, Wang S, et al. LncRNA SNHG17 promotes gastric cancer progression by epigenetically silencing of p15 and p57. J Cell Physiol. 2019;234:5163–5174.

[25] Ma Z, Gu S, Song M, et al. Long non-coding RNA SNHG17 is an unfavourable prognostic factor and promotes cell proliferation by epigenetically silencing P57 in colorectal cancer. Mol Biosyst. 2017;13:2350–2361.

[26] Xu T, Yan S, Jiang L, et al. Gene amplification-driven long noncoding RNA SNHG17 regulates cell proliferation and migration in human non-small-cell lung cancer. Mol Ther Nucleic Acids. 2019;17:405–413.

[27] Livak KJ, Schmittgen TD. Analysis of relative gene expression data using real-time quantitative PCR and the 2(-Delta Delta C(T)) Method. Methods. 2001;25:402–408.

[28] Klec C, Prinz F, Pichler M. Involvement of the long non-coding RNA NEAT1 in carcinogenesis. Mol Oncol. 2019;13:46–60.

[29] Xu Q, Zhu Q, Zhou Z, et al. MicroRNA-876-5p inhibits epithelial-mesenchymal transition and metastasis of hepatocellular carcinoma by targeting BCL6 corepressor like 1. Biomed Pharmacothe. 2018;103:645–652.

[30] Xu J, Zheng J, Wang J, et al. miR-876-5p suppresses breast cancer progression through targeting TFAP2A. Exp Ther Med. 2019;18:1458–1464.

[31] Li T, Li Y, Sun H. MicroRNA-876 is sponged by long noncoding RNA LINC00707 and directly targets metadherin to inhibit breast cancer malignancy. Cancer Manag Res. 2019;11:5255–5269.

[32] Xu Z, Yu Z, Tan Q, et al. MiR-876-5p regulates gastric cancer cell proliferation, apoptosis and migration through targeting WNT5A and MITF. Biosci Rep. 2019 Jun 28;39(6). pii: BSR20190066. doi: 10.1042/BSR20190066. Print 2019 Jun 28.

[33] Xie W, Xiao J, Wang T, et al. MicroRNA-876-5p inhibits cell proliferation, migration and invasion by targeting c-Met in osteosarcoma. J Cell Mol Med. 2019;23:3293–3301.

[34] Bao L, Lv L, Feng J, et al. MiR-876-5p suppresses epithelial-mesenchymal transition of lung cancer by directly down-regulating bone morphogenetic protein 4. J Biosci. 2017;42:671–681.

[35] Li ZQ, Zou R, Ouyang KX, et al. An in vitro study of the long non-coding RNA TUG1 in tongue squamous cell carcinoma. J Oral Pathol Med. 2017;46:956–960.

[36] Yu J, Liu Y, Guo C, et al. Upregulated long non-coding RNA LINC00152 expression is associated with progression and poor prognosis of tongue squamous cell carcinoma. J Cancer. 2017;8:523–530.

[37] Yu J, Liu Y, Gong Z, et al. Overexpression long non-coding RNA LINC00673 is associated with poor prognosis and promotes invasion and metastasis in tongue squamous cell carcinoma. Oncotarget. 2017;8:16621–16632.

[38] Ouyang KX, Zou R, Liang J, et al. TUC338 overexpression leads to enhanced proliferation and reduced apoptosis in tongue squamous cell carcinoma cells in vitro. J Oral Maxillofacial Surg. 2017;75:423–428.

[39] Huang W, Cui X, Chen J, et al. Long non-coding RNA NKILA inhibits migration and invasion of tongue squamous cell carcinoma cells via suppressing epithelial-mesenchymal transition. Oncotarget. 2016;7:62520–62532.

[40] Yang YT, Wang YF, Lai JY, et al. Long non-coding RNA UCA1 contributes to the progression of oral squamous cell carcinoma by regulating the WNT/beta-catenin signaling pathway. Cancer Sci. 2016;107:1581–1589.

[41] Chang WC, Hung JJ. Functional role of post-translational modifications of Sp1 in tumorigenesis. J Biomed Sci. 2012;19:94.

[42] Davie JR, He S, Li L, et al. Nuclear organization and chromatin dynamics–Sp1, Sp3 and histone deacetylases. Adv Enzyme Regul. 2008;48:189–208.

[43] Sankpal UT, Goodison S, Abdelrahim M, et al. Targeting Sp1 transcription factors in prostate cancer therapy. Med Chem. 2011;7:518–525.

[44] Yue L, Li L, Liu F, et al. The oncoprotein HBXIP activates transcriptional coregulatory protein LMO4 via Sp1 to promote proliferation of breast cancer cells. Carcinogenesis. 2013;34:927–935.

[45] Xu Y, Zhao F, Wang Z, et al. MicroRNA-335 acts as a metastasis suppressor in gastric cancer by targeting Bcl-w and specificity protein 1. Oncogene. 2012;31:1398–1407.

[46] Yan DG, Liu N, Chao M, et al. SP1-induced upregulation of long noncoding RNA LINC00313 contributes to papillary thyroid cancer progression via the miR-422a. Eur Rev Med Pharmacol Sci. 2019;23:1134–1144.

[47] Jia LF, Huang YP, Zheng YF, et al. miR-29b suppresses proliferation, migration, and invasion of tongue squamous cell carcinoma through PTEN-AKT signaling pathway by targeting Sp1. Oral Oncol. 2014;50:1062–1071.

[48] Jia L, Huang Y, Zheng Y, et al. miR-375 inhibits cell growth and correlates with clinical outcomes in tongue squamous cell carcinoma. Oncol Rep. 2015;33:2061–2071.

[49] Sun L, Liang J, Wang Q, et al. MicroRNA-137 suppresses tongue squamous carcinoma cell proliferation, migration and invasion. Cell Prolif. 2016;49:628–635.